SCALING OF PERMEABILITIES AND FRICTION FACTORS OF HOMOGENEOUSLY EXPANDING GAS-SOLIDS FLUIDIZED BEDS
Geldart's A powders and magnetically stabilized beds

by

Jordan Y. HRISTOV

Original scientific paper
UDC: 533.6.011:519.876.5–912
BIBLID: 0354-9836, *10* (2006), 1, 19-44

The concept of a variable friction factor of fluid-driven deformable powder beds undergoing fluidization is discussed. The special problem discussed addresses the friction factor and bed permeability relationships of Geldart's A powders and magnetically stabilized beds in axial fields. Governing equations and scaling relationships are developed through three approaches: (1) Minimization of the pressure drop with respect to the fluid velocity employing the Darcy-Forchheimer equation together with the Richardson-Zaki scaling law, (2) Minimization of the pressure drop across an equivalent-channel replacing the actual packed beds by a straight pipe with bed-equivalent obstacle of a simple geometry, and (3) Entropy minimization method applied in cases of the Darcy-Forchheimer equation and the equivalent-channel model. Bed-to-surface heat transfer coefficients are commented in the context of the porosity/length scale relationships developed.
Both the pressure drop curves developments and phase diagram designs are illustrated by applications of the intersection of asymptotes technique to beds exhibiting certain degree of cohesion.

Key words: *fluidization, magnetic field stabilized bed, friction factor, permeability, scaling, Richardson-Zaki law, Darcy-Forchheimer equation, entropy minimization method, bed-to surface heat transfer, intersection of asymptotes technique*

Introduction

Permeabilities and friction factors of homogeneously expanding gas-fluidized beds such as Geldart's' A powders [1] and magnetically stabilized beds [2, 3] in axial fields are at issue. The problems are considered here from a general point view regarding minimization of the pressure drop across the bed during the fluid-driven deformation, *i. e*. beyond the minimum fluidization point. The discussion began in the previous study [4] where experimental results and Richardson-Zaki law allowed to estimate *porosity* / *friction factor* scaling relationships. These results will be commented briefly below for clarity of further explanations.

Briefs of the previous results 4

The magnetic field assisted fluidization (MFAF) considers fluidization of magnetic solids controlled by external magnetic fields [2, 3]. The discussion is focussed on a state termed "magnetically stabilized bed" (MSB) [2-4]. Generally, MSB expands due to fluid drag forces [2, 4], *i. e*. it is a packed bed (porous medium) with a deformable structure. The stabilized beds exhibit two types of pressure drop curves during the fluid-driven expansion (deformation) – flat pressure drop profiles that implies a fluid velocity independent pressure drop (see fig. 1a) and decreasing pressure drop (fig. 1b). The former case dominates in the literature since most of the studies consider fluidization of A powders or beds stabilized by axial magnetic fields [1, 3-5]. Bed stabilizations by external fields with orientations different from axial are special cases that will be commented briefly at the end of this paper. These behaviours were discussed in [4] from the viewpoint of a fluid-dependent hydraulic resistance of the bed. Moreover, it was pointed that bed stabilized by axial fields exhibit negative differential hydraulic resistances. The results obtained in [4] will be briefly outlined below for clarity of the present discussion.

The analysis of the friction factor of the equation (pipe flow analogy) [4]:

$$\Delta P \quad C_D \frac{L}{d_\mathrm{p}} \frac{\rho U^2}{2} \tag{1}$$

leads to the fact that the ratio $R_c = C_\mathrm{i}/C_0$ (at $H = 0$ and $U = U_{e1}$) is a function of the dimensionless gas velocity, U/U_{mf0}, *i. e*. $R_c = C_\mathrm{i}/C_0 =$ (U/U_{mf0}) correlates approximately as $R_c = 1.02(U/U_{mf0})^{-2.25}$. Further it was accepted that R_c $(U/U_{mf0})^{-2}$ for convention with the well-known equations, such as eq. (1). In other words, the friction factor decreases faster ($1/\mathrm{Re}_\mathrm{p}^2$) unlike the classical non-deformable granular beds ($1/\mathrm{Re}_\mathrm{p}$), due to bed deformable structure.

The well known one-dimensional Forchheimer equation of a fluid flow through a saturated porous medium [6, 7] is :

$$\frac{\Delta P}{L} \quad \frac{\mu}{K} U \quad \frac{F\rho_\mathrm{g}}{\sqrt{K}} U^2 \tag{2}$$

It was employed to derive a scaling relationship between the permeability and porosity under the following conditions:

(1) a *constant pressure drop* (P)/ $U = 0$, and
(2) Richardson-Zaki scaling law U/U_t ε^n is valid in cases of magnetically stabilized beds [2].

The result developed in [4] is:

$$K \quad \frac{1}{F}\frac{\mu}{\rho}\frac{1}{U}^2 \quad \frac{\varepsilon}{n(1 \quad \varepsilon) \quad \varepsilon}^2 \quad \frac{1}{F}\frac{\mu}{\rho}\frac{1}{U}^2 \Phi(\varepsilon) \tag{3}$$

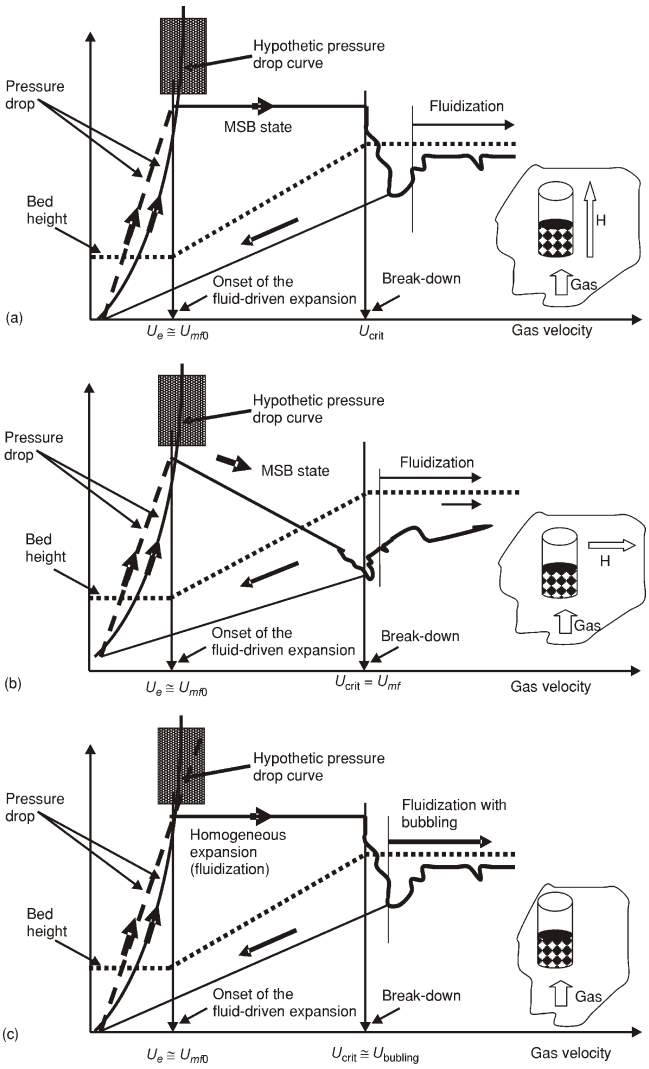

Figure 1. Typical pressure drop and bed expansion curves (schematically) of magnetically stabilized beds fluidized by gas. The insets show schematically the experimental situations (see insets, the vertical arrows H denote the magnetic field); *(a) in an axial field (see inset), (b) in a transverse field (see inset), and (c) fluidization of A powders according to Geldart (see inset)*

Common comments:
The velocity range U U_e U_{mf0} corresponds to a fixed non-deformable bed. The dotted line presents the usual approximation. The solid line represents an actual pressure drop curve described by two-term equation such as the Darcy-Forchheimer one discussed in the present paper. The part denoted as a hypothetic one represent what the pressure drop across the bed would if the bed would not expand at U = U_e. This line is commented further in the text of the present paper as the first asymptotes of the pressure drop

In a simplified form (especially for) and taking into account the range of porosity variations 0.4 ε 0.8, the corresponding porosity function and friction factor are :

$$\Phi(\varepsilon) \quad \frac{1}{n}\varepsilon^{(n\ 1)} \qquad f \quad 1 \quad \frac{n}{\varepsilon} \quad 1 \quad \frac{n_0 \quad p \quad \frac{H}{Ms}}{\varepsilon} \tag{4}$$

where the nominator of the second expression of eq. (4) represents the magnetic field effect on the Richardson-Zaki exponent [3], namely:

$$n \quad n_0 \quad p \quad \frac{H}{Ms} \tag{5}$$

Problem formulations

The application of the Darcy-Forchheimer equation in its general form eq. (2) to deformable particle bed gives rise to several general questions:

(1) Is it possible to derive functional relationship concerning bed permeability and the overall bed porosity if the bed expands (fluid-driven expansion) and the Richardson--Zaki law is valid?
(2) Is it possible to derive *porosity* / *friction factor* functional relationships employing equivalent mechanical models?
(3) Is it possible to apply the entropy minimization method [8] for defining *porosity/permeability* functional relationships in case of deformable beds?
(4) The above questions are general and address fluidization of particulate beds with significant degree of cohesion that is bed behaviour defined by the Geldart's group A [1]. Since the magnetically stabilized in axial fields exhibit such A behaviour, the reasonable questions are: (a) how the magnetic field affects the bed frictional resistance; (b) how the bed permeability is affected by the external field intensity and orientation; and (c) how the bed-to-surface heat transfer coefficient is related to the bed porosity change and how the field can control it.
(5) Does the method of intersection of asymptotes developed by Bejan [9] works in cases of homogeneously expanding gas-fluidized beds.

Methodology of the study

The formulated on before problems need some preliminary comments with reference to the methodologies and techniques used for their solutions. Several methods are applied to study different problems of the bed fluid driven deformation and the relevant friction factors. First, the study begins with the Darcy-Forchheimer equation and addresses the functional relationship between the bed permeability and the overall porosity if the pressure drop is fluid velocity-independent. The second approach replaces the ac-

tual porous bed by an *equivalent-channel model and* derives friction factor correlations relevant to the fluid-driven deformations of the real particle bed. Third, a special attempt is made to apply the Bejan's *method of entropy minimisation* for deriving the required functional porosity/friction factor relationships. Since this method uses more general thermodynamic basis than the first two approaches, the results from its application give additional universal information permitting to comment basic elements of bed behaviour undergoing fluidization. The fourth method applied to explain the effect of the interparticle forces on the pressure drop curves is the Bejan's *intersection of asymptotes technique* [9].

Final targets of the study

These special comments address both the final users interested in useful engineering equations and those attracted by theory developments. The practical reason for the study is the need to calculate the pumping power for fluidized beds where the interparticle forces dominate and control the bed behaviour. Moreover, the results developed are functional relationships that can be directly applied to actual situations. The theoretical tasks are to see the bed as a self-organizing system and how the general thermodynamic methods can explain some crucial points of bed behaviour.

Direct analysis of Darcy-Forchheimer equation

Consider the Darcy-Forchheimer equation expressed by eq. (2) . Since the process is a fluid-driven deformation all the coefficients are fluid velocity dependent values, *i. e.* $K = K(\varepsilon)$ and $\varepsilon = \varepsilon(U)$. The complete derivative of eq. (2) with respect the velocity U and setting $P/\ U = 0$ yield:

$$0 \quad \frac{\mu}{K}U \quad \frac{F\rho_g}{\sqrt{K}}U^2 \quad \frac{\partial L_i}{\partial U} \quad \frac{L_i}{U} \quad \frac{1}{K}\frac{\partial K}{\partial \varepsilon_i}\frac{\partial \varepsilon_i}{\partial U} \tag{6}$$

Taking into account that the first term in brackets of eq. (6) is not zero (*see the note at end of this section*) and performing rearrangement of the second term of eq. (6) we read:

$$\frac{1}{K}\frac{\partial K}{\partial \varepsilon_i} \quad \frac{1}{L}\frac{\partial L_i}{\partial \varepsilon_i} \quad \frac{1}{U}\frac{\partial U}{\partial \varepsilon_i} \tag{7}$$

According to the Richardson-Zaki law and the solid mass conservation equation $L_i(1 - \varepsilon_i) = L_0(1 - \varepsilon_0)$ we read:

$$\frac{1}{U}\frac{\partial U}{\partial \varepsilon_i} \quad \frac{n}{\varepsilon_i} \quad \text{and} \quad \frac{\partial L_i}{\partial \varepsilon_i} \quad L_0\frac{1 \quad \varepsilon_0}{(1 \quad \varepsilon_i)^2} \tag{8}$$

Substitution of eq. (8) into eq. (7) yields:

$$\frac{\mathrm{d}K}{K} \quad \frac{n}{\varepsilon_\mathrm{i}} \quad \frac{1}{1 \quad \varepsilon_\mathrm{i}} \quad \mathrm{d}\varepsilon \tag{9}$$

The initial condition defines $K_0 = K(\varepsilon_0)$ at $\varepsilon = \varepsilon_0$, where K_0 can be determined by a simple techniques of linearization [6] of eq. (2) in the form $-(\Delta P/L)(1/U) = (\mu/K) + (F\rho_\mathrm{g}/K^{1/2})U$ or through the Ergun's correlation [10, 11] as $K_0 \quad \varepsilon_0^3 d_\mathrm{p}^2 / 150(1 \quad \varepsilon_0)^2$ with $F \quad 1.75 / 150^{1/2} \varepsilon_0^{3/2}$. The solution of eq. (9) is:

$$\frac{K_\mathrm{i}}{K_0} \quad \frac{\varepsilon_\mathrm{i}}{\varepsilon_0} \quad ^n \frac{1 \quad \varepsilon_\mathrm{i}}{1 \quad \varepsilon_0} \tag{10a}$$

In general the *permeability/porosity* function expressed as:

$$K \quad \frac{\varepsilon^n}{1 \quad \varepsilon} \tag{10b}$$

resembles the porosity function used in the Ergun's correlation (see eq. 49).

The corresponding friction factor takes the form:

$$f \quad \frac{1}{\mathrm{Re}} \quad 1 \quad \frac{1}{\dfrac{\rho_\mathrm{g} U \sqrt{K}}{\mu}} \quad 1 \quad \sqrt{\frac{1 \quad \varepsilon}{\varepsilon^{3n}}} \quad 1 \tag{11}$$

Hence, the friction factor decreases with increasing bed porosity that is physically correct.

Note: Equation (6) provides an alternative solution if the first term in the brackets is equal to zero. There exist two unrealistic roots: $U_1 = 0$ and $U_2 = -\mu/F\rho\sqrt{K}$.

Equivalent "channel" model

The porous media fluid flow has been modelled trough various equivalent hydraulic structures [12]. Such an example is the Kozeny-Carman equation developed on the basis of the Hagen-Poiseuille flow through parallel capillaries [13, 14]. The following analysis is provoked by the ideas of Lage [15, 16] investigating the minimum pressure drop across a porous sample enough to apply correctly the Hagen-Dupuit-Darcy equation. The slot model proposed by Lage [15] implies replacement of a porous medium by an equivalent slot formed by parallel plates with variable distance and length (see fig. 2a). According to the analysis performed in [15] the fluid flow is determined by:

$$U(X,Y) \quad \frac{64\mathrm{Re}}{H^2} \quad \frac{H}{2}^2 \quad Y^2 \tag{12}$$

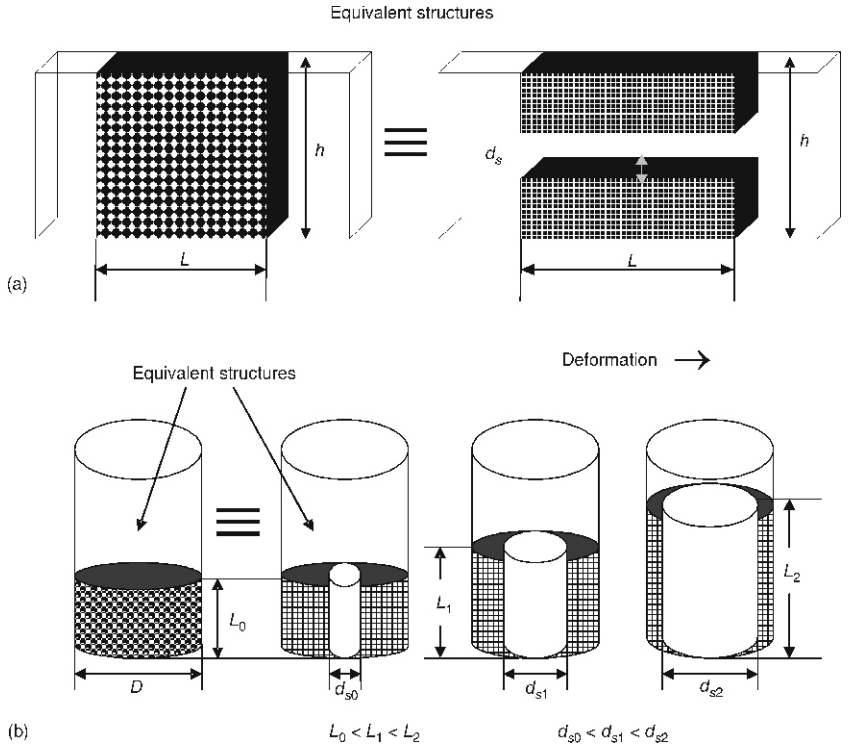

Figure 2. Equivalent hydraulic models of a porous bed
(a) Lage's equivalent "slot" model [15]; (b) Present equivalent "channel" model

where $H = h/d_s$ is the dimensionless channel length and Re $\overline{u}_i h/\nu$ $\overline{u}_s d_s/\nu$ is the Reynolds number for both the channel and the slot. The slotted plate being a constrain to flow is considered as a porous medium having (surface) porosity ε defined as:

$$\varepsilon \quad \frac{d_s}{h} \quad \frac{1}{H} \tag{13}$$

Now, consider a packed bed confined by a circular tube that can be replaced by an equivalent-channel illustrated in fig. 2b. The solid phase volume is equal to that of the cylindrical shell, while the free volume (bed voidage) is equivalent to the core cylinder volume of diameter d_s.

$$V_{\text{bed0}} \quad \pi\frac{D^2}{4}L_0, \quad V_0 \quad \varepsilon_0 V_{\text{bed0}} \quad \text{and} \quad V_0 \quad \pi\frac{d_s^2}{4}L_0 \tag{14}$$

The relationships (14) defines the slot porosity as:

$$\varepsilon \quad \frac{d_s}{D}^2 \tag{15}$$

The definition (15) differs from (13) due to the cylindrical geometry of the equivalent hydraulic structure. At each step of the bed deformation we may define an equivalent channel with a pressure drop expressed by eq. (1), namely:

– initial bed, at $U = U_e$ $\Delta P_0 \quad f_0 \frac{L_0}{d_{s0}} \frac{\rho U_e^2}{2}$ (16a)

and

– deformable bed, at $U_i \quad U_e$ $\Delta P_i \quad f_i \frac{L_i}{d_{si}} \frac{\rho U_i^2}{2}$ (16b)

where $U_i \quad U_e$.

In eq. (16a) we assume that the reference friction factor is that at $U = U_e$ since beyond this point the bed deformation begins. The second important condition is the constant pressure drop across the channel (core cylinder), that is:

$$\Delta P_i = \Delta P_0 \tag{17a}$$

$$f_0 \frac{L_0}{d_{s0}} \frac{\rho U_{se}^2}{2} \quad f_i \frac{L_i}{d_{si}} \frac{\rho U_{si}^2}{2} \tag{17b}$$

where U_{se} and U_{si} are superficial fluid flow velocity in the core with a diameter d_s.

The relationship with the velocities defined by the tube diameter D is:

$$U_{si} \quad \frac{U_i}{\varepsilon^2} \tag{18}$$

since from eq. (15) we have $d_s/D = \sqrt{\varepsilon}$

The friction factor ratio can be expressed as:

$$\frac{f_i}{f_0} \quad \frac{U_{se}}{U_{si}}^2 \frac{L_0}{L_i} \frac{d_{si}}{d_{s0}} \tag{19}$$

where the subscript 0 denotes the quantities corresponding to the reference bed state at $U = U_e$ and $\varepsilon = \varepsilon_0$, *i. e.* f_0 is the reference friction factor.

For a packed bed the solids mass conservation defines $L_0/L_i = (1 - \varepsilon)/(1 - \varepsilon_0)$. Further, the Richardson-Zaki law is valid, so taking into account eq. (18) we can read eq. (19) as:

$$\frac{f_i}{f_0} \quad \frac{\varepsilon_i}{\varepsilon_0} \quad \frac{\varepsilon_0}{\varepsilon_i}^n \sqrt{\varepsilon} \frac{1 \quad \varepsilon_i}{1 \quad \varepsilon_0} \quad f_i \quad f_0 \frac{1 \quad \varepsilon_i}{\varepsilon_i^{n \quad \frac{3}{2}}} \frac{\varepsilon_0^{n \quad 1}}{1 \quad \varepsilon_0} \tag{20}$$

Hence, f_i decreases with increasing porosity, as expected. This result can be compared directly with the friction factor relationship for a Darcy-Forchheimer porous

medium, eq. (4), *i. e.* f_{i} (1 / Re) 1as commented in [4]. The friction factor ratio eq. (20) in this case yields:

$$f_{\mathrm{i}} \quad f_0 \sqrt{\frac{1 \quad \varepsilon_{\mathrm{i}}}{\varepsilon_{\mathrm{i}}^n}} \sqrt{\frac{\varepsilon_0^n}{1 \quad \varepsilon_0}} \tag{21a}$$

From its equivalent form eq. (4b) f_{i} 1 (n/ε) we read:

$$f_{\mathrm{i}} \quad f_0 \; 1 \quad \frac{n}{\varepsilon} \tag{21b}$$

All these functional relationships seem different, that is a reasonable effect of the differences in the models applied for their development. However, taking into account that the mean value of n can be assumed as n 3, both eqs. (20) and (21a) yield $n/2 = n - 3/2 = 1.5$. Hence, for moderate bed deformation these scaling relationships give almost equal results.

Bed-to-surface heat transfer coefficients-scaling from the slot model

Consider bed-to-surface heat transfer in a case of an immersed surface and a stabilized bed. As commented in [4, 10] the bed heat conductivity can be neglected and only gas convection contributes the heat transfer. Hence, in the equivalent channel model, the bed-to-surface heat transfers can be modelled by a body (surface) imbedded in the channel. The simplest case is plate parallel to the slot walls and streamlined by the flow. The Nusselt number power-law relationship in it general form is:

$$\mathrm{Nu} \quad A\,\mathrm{Re}^{\,p}\,\mathrm{Pr}^{\,q} \tag{22a}$$

where $\mathrm{Re} = \mathrm{Re}_{\mathrm{s}}$ for the channel is defined as in eq. (12).

For the equivalent hydraulic structures defined above the Nusselt number ratio can be expressed as:

$$\frac{\mathrm{Nu}_{\mathrm{i}}}{\mathrm{Nu}_0} \quad \frac{\mathrm{Re}_{\mathrm{i}}}{\mathrm{Re}_0}^{\,p} \quad \frac{\mathrm{Nu}_{\mathrm{i}}}{\mathrm{Nu}_0} \quad \frac{U_{si}}{U_{se}}^{\,p} \tag{22b}$$

Taking into account the relationships (15) and (18) we read:

$$\frac{\mathrm{Nu}_{\mathrm{i}}}{\mathrm{Nu}_0} \quad \frac{\varepsilon_0}{\varepsilon_i}^{\,2} \frac{U_{si}}{U_{se}} \quad \frac{\mathrm{Nu}_{\mathrm{i}}}{\mathrm{Nu}_0} \quad \frac{\varepsilon_0}{\varepsilon_i}^{\,2} \quad \frac{\varepsilon_{\mathrm{i}}}{\varepsilon_0}^{\,n} \tag{23a}$$

$$\frac{h_{\mathrm{Wi}}}{h_{\mathrm{W}\,0}} \quad \frac{\varepsilon_{\mathrm{i}}}{\varepsilon_0}^{\,n\;2} \tag{23b}$$

Hence, the value of h_{Wi} decreases as the exponent n is decreased (due to the field effect) and increases as the porosity is increased, as proved in [4, 10].

Entropy generation minimization approach

Following the main idea of the journal issues dedicated to Adrian Bejan, the analysis developed below is based on the entropy generation minimization. In general, a homogenously expanded fluidized bed (behaviour of A Geldart's powder or a magnetically stabilized bed) is a porous medium confined by tube walls, so it may be considered as a specific obstacle to the fluid flow with defined pressure drop and friction factor respectively. Consider the bed illustrated in fig. 3 and a constant heat flux q is imposed on its surface. Fluid with a mass flow rate $\dot{m}$ and inlet temperature T_0 enters the tube (the bed) of length L. The rate of heat transfer to the fluid (bed) inside the control volume is:

$$\delta\dot{Q} \quad \dot{m}C_{\mathrm{p}}\mathrm{d}T \quad q\ \pi D\mathrm{d}x \tag{24a}$$

where

$$\dot{m} \quad \rho U\frac{\pi D^2}{4} \tag{24b}$$

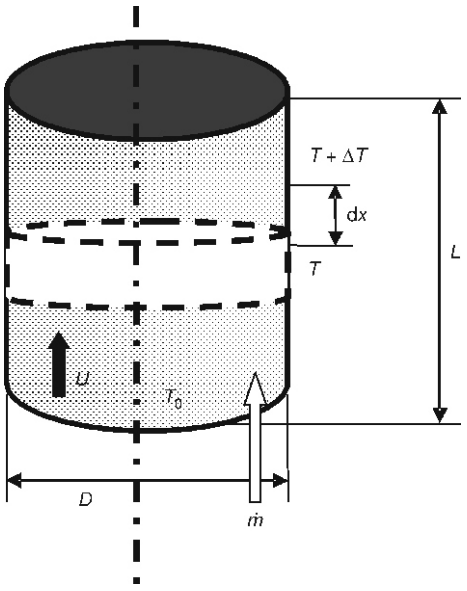

Figure 3. Schematic presentation of the bed (confined by a tube of diameter *D*) used to derive the entropy generation – eq.

The total entropy generation within the control volume in fig. 3 may be written as:

$$\mathrm{d}\dot{S}_{\mathrm{gen}} \quad \dot{m}\mathrm{d}s \quad \frac{\delta\dot{Q}}{T_{\mathrm{W}}} \tag{25}$$

where, for an incompressible fluid:

$$\mathrm{d}s \quad C_{\mathrm{p}}\frac{\mathrm{d}T}{T} \quad \frac{\mathrm{d}P}{\rho T} \tag{26}$$

Substituting eqs. (25) and (26) into eq. (24a) we read:

$$\mathrm{d}\dot{S}_{gen} \quad \dot{m}C_{\mathrm{p}}\ \frac{T_{\mathrm{W}} \quad T}{TT_{\mathrm{W}}}\mathrm{d}T \quad \frac{1}{\rho C_{\mathrm{p}}T}\mathrm{d}P \tag{27}$$

In absence of a heat flux the first term of eq. (26) drops and we have only entropy generation due to viscous flow dissipation:

$$\mathrm{d}s \quad \frac{\mathrm{d}P}{\rho T} \tag{28a}$$

$$\mathrm{d}\dot{S}_{\mathrm{gen}} \quad \dot{m}\frac{1}{\rho T}\mathrm{d}P \tag{28b}$$

The general question investigated below considers entropy minimization with a pressure drop (across the porous bed) represented by several models: (1) Darcy--Forchheimer equation, and (2) Hagen-Dupuit-Darcy equation in two cases: equivalent channel model, and (3) the models following from eq. (1) .

Darcy-Forchheimer equation

Assuming the pressure drop across the control volume of the bed expressed by eq. (2) $-\mathrm{d}P = (\mu/K)U + (F\rho/K^{1/2})U^2$ and the mass flow rate. The entropy generation rate according to eq. (24b) is:

$$\mathrm{d}\dot{S}_{\mathrm{gen}} \quad \frac{\pi D^2}{4}\frac{1}{T}U \quad \frac{\mu}{K}U \quad \frac{F\rho}{\sqrt{K}}U^2 \quad \mathrm{d}x \tag{29}$$

Integrating eq. (29) along the bed length the total entropy generation in the bed becomes:

$$\dot{S}_{\mathrm{gen}} \quad \frac{\pi D^2}{4}\frac{1}{T}U \quad \frac{\mu}{K}U \quad \frac{F\rho}{\sqrt{K}}U^2 \quad L \tag{30a}$$

and an entropy generation ratio can be defined as:

$$N_{S1} \quad \frac{\dot{S}_{\mathrm{gen}}}{\dot{S}_{\mathrm{gen}\,0}} \tag{30b}$$

where the $\dot{S}_{\mathrm{gen}\,0}$ corresponds to the non-deformed bed.

Consider a bed deformation with a fluid flow-dependent permeability. The entropy generation rate is a measure of the available work during the fluid flow through the deformable porous matrix. The bed expansion is a form of a particle self-organization process that minimizes the bed resistance. Therefore, if we think about the problem of the entropy minimization we might find out what would be the porous medium behaviour satisfying such a condition. The derivative of eq. (30a) with respect to the fluid velocity (see for similar differentiation of LHS of eq. (30a) in [4]) may be set equal to zero as a condition for a minimum of the function, so:

$$\frac{\mathrm{d}\dot{S}_{\mathrm{gen}}}{\mathrm{d}U} \quad \frac{\pi D^2}{4}\frac{1}{T} \quad \frac{1}{\mathrm{Re}} \quad 1 \quad U\frac{\partial L}{\partial U} \quad L \quad 2 \quad \frac{U}{K} \quad \frac{\partial K}{\partial \varepsilon}\frac{\partial \varepsilon}{\partial U} \quad L \quad 0 \tag{31}$$

Assuming that the bed operates at Re > 1 it follows that 1 + 1/Re 1, so eq. (31) yields:

$$\frac{1}{K}\frac{\partial K}{\partial \varepsilon} \quad 3 \quad \frac{U}{L}\frac{\partial L}{\partial U} \quad \frac{1}{U}\frac{\partial U}{\partial \varepsilon} \tag{32}$$

From the Richardson-Zaki law and the solid mass conservation – see for these transformations in [4] and eq. (8) here – we have $(1/U)(\ U/\ \varepsilon) = n/\varepsilon$ and $\partial L/\partial U =$ $(\partial L/\partial \varepsilon)(\partial \varepsilon/\partial U)$ $(\partial \varepsilon/\partial U)[-L_0(1-\varepsilon_0)/(1-\varepsilon)^2]$. Hence, eq. (32) becomes:

$$\frac{1}{K}\frac{\partial K}{\partial \varepsilon} \quad 3\frac{n}{\varepsilon} \quad \frac{1}{1 \quad \varepsilon} \tag{33}$$

The solution of eq. (33) with an initial condition $K = K_0$ at $\varepsilon = \varepsilon_0$ yields:

$$\frac{K}{K_0} \quad \frac{\varepsilon}{\varepsilon_0}^{3n} \quad \frac{1 \quad \varepsilon}{1 \quad \varepsilon_0} \tag{34a}$$

Consider eq. (31) and denoting $R = (1/\mathrm{Re}) + 1$ the general form of the solution becomes:

$$\frac{K}{K_0} \quad \frac{\varepsilon}{\varepsilon_0}^{2\ \frac{1}{R}\ n} \quad \frac{1 \quad \varepsilon}{1 \quad \varepsilon_0} \tag{34b}$$

Similar solution with and an exponent n instead $3n$ was derived in [4] from the condition of fluid velocity-independent pressure drop $\partial P/\partial U$ 0. Irrespective of the form of the exponent the differential equations developed in both cases ($\partial P/\partial U$ 0 and $\mathrm{d}\dot{S}_{\mathrm{gen}}/\mathrm{d}U$ 0) have almost equal structures and solutions. Therefore, we may decide that the condition of entropy generation minimization has its macroscopic performance in the particle packing self-organization presented by constant pressure drop maintenance across the deformable bed.

Moreover, the permeability/porosity functions (34a and b) ensure that the entropy generation ratio:

$$N_{S1} \quad \frac{\varepsilon_0}{\varepsilon}^{n} \quad \frac{1 \quad \varepsilon}{1 \quad \varepsilon_0} \quad 1 \tag{35}$$

through the fluid-driven deformation of the porous bed.

Equivalent channel model – entropy minimization approach

The equivalent channel model is considered again from the standpoint of the entropy generation minimization. Consider the pressure drop across the equivalent slot in

the form expressed by eq. (16b) and substitute it into eq. (28b) taking into account eqs. (24a) and (18). The entropy generation rate for the control volume of the slot is:

$$\mathrm{d}\dot{S}_{\mathrm{gen}} \quad f_{\mathrm{i}} \quad \frac{1}{d_{s\mathrm{i}}} \frac{\rho U_{s\mathrm{i}}^{2}}{2} U_{s\mathrm{i}} \varepsilon^{2} \quad \mathrm{d}x \tag{36a}$$

Integration of eq. (36a) along the core cylinder length L yields:

$$\dot{S}_{\mathrm{gen}} \quad f_{\mathrm{i}} \quad \frac{1}{d_{s\mathrm{i}}} \frac{\rho U_{s\mathrm{i}}^{3}}{2} \varepsilon^{2} \quad L \tag{36b}$$

The ratio of the entropy generation rates for the velocities U_{i} and U_0 (reference velocity corresponding to non-deformed bed) is:

$$N_{S2} \quad \frac{\dot{S}_{\mathrm{gen}}}{\dot{S}_{\mathrm{gen}\,0}} \quad \frac{f_{\mathrm{i}}}{f_0} \frac{d_{s0}}{d_{s\mathrm{i}}} \quad \frac{U_{s\mathrm{i}}}{U_{s0}} \quad ^{3} \quad \frac{\varepsilon_{\mathrm{i}}}{\varepsilon_0} \quad ^{2} \frac{L_{\mathrm{i}}}{L_0} \tag{37a}$$

Taking into consideration the solid mass conservation ratio as well $d_{s0}/d_{s\mathrm{i}} = (\varepsilon_0/\varepsilon_{\mathrm{i}})^2$ and the relationship (18) the dimensionless ratio $\dot{S}_{\mathrm{gen}} / \dot{S}_{\mathrm{gen}\,0}$ reads:

$$\frac{\dot{S}_{\mathrm{gen}}}{\dot{S}_{\mathrm{gen}\,0}} \quad \frac{f_{\mathrm{i}}}{f_0} \quad \frac{\varepsilon_0}{\varepsilon_{\mathrm{i}}} \quad ^{2} \quad \frac{\varepsilon_{\mathrm{i}}}{\varepsilon_0} \quad ^{3(n\ 1)} \quad \frac{\varepsilon_{\mathrm{i}}}{\varepsilon_0} \frac{1\ \ \varepsilon_0}{1\ \ \varepsilon_i} \quad \frac{f_{\mathrm{i}}}{f_0} \quad \frac{\varepsilon_{\mathrm{i}}}{\varepsilon_0} \quad ^{3n\ \ 4} \frac{1\ \ \varepsilon_0}{1\ \ \varepsilon_{\mathrm{i}}} \tag{37b}$$

Differentiation of RHS of eq. (37b) with respect to the porosity ε_{i} yields:

$$\frac{\mathrm{d}}{\mathrm{d}\varepsilon_{\mathrm{i}}} \quad \frac{\dot{S}_{\mathrm{gen}}}{\dot{S}_{\mathrm{gen}\,0}} \quad \frac{\varepsilon_{\mathrm{i}}}{\varepsilon_0} \quad ^{3n\ \ 4} \frac{1\ \ \varepsilon_0}{1\ \ \varepsilon_{\mathrm{i}}} \quad \frac{1}{f_0} \frac{\mathrm{d}f_{\mathrm{i}}}{\mathrm{d}\varepsilon_{\mathrm{i}}} \quad \frac{f_{\mathrm{i}}}{f_0} \quad \frac{3n\ \ 4}{\varepsilon_i} \quad \frac{1}{1\ \ \varepsilon_{\mathrm{i}}} \tag{38}$$

The condition $\mathrm{d}\dot{S}_{\mathrm{gen}} / \mathrm{d}\varepsilon_{\mathrm{i}} = 0$ yields:

$$\frac{\mathrm{d}\ \ \frac{f_{\mathrm{i}}}{f_0}}{\mathrm{d}\varepsilon_{\mathrm{i}}} \quad \frac{f_{\mathrm{i}}}{f_0} \quad \frac{1}{1\ \ \varepsilon_{\mathrm{i}}} \quad \frac{3n\ \ 4}{\varepsilon_{\mathrm{i}}} \tag{39}$$

The solution of eq. (39) with the initial condition $f_{\mathrm{i}} = f_0$ at $\varepsilon_{\mathrm{i}} = \varepsilon_0$ is:

$$\frac{f_{\mathrm{i}}}{f_0} \quad \frac{\varepsilon_0}{\varepsilon_{\mathrm{i}}} \quad ^{3n\ \ 4} \frac{1\ \ \varepsilon_{\mathrm{i}}}{1\ \ \varepsilon_0} \tag{40a}$$

That is, the friction factor/porosity function is:

$$f_{\mathrm{i}} \quad \frac{1\ \ \varepsilon}{\varepsilon} \tag{40b}$$

A backward glance on eq. (37a) shows that $N_{S2} < 1$ if the porosity function (40b) is satisfied, namely the functional relationship (40b) ensures entropy minimization during a fluid-driven bed deformation.

Pipe equation (1) – entropy minimization approach

The pipe equtation (1) was investigated in [4] and a scaling relationship concerning the evolution of the internal bed length scale d_p was developed as:

$$d_c \quad d_p \varepsilon^n \tag{41}$$

where d_c is the internal length scale of the deformable bed, while the particle diameter d_p is the reference length scale of the non-deformed bed. Consider the ratio of the entropies generated (see eq. 28b) trough the fluid flow in both the fixed and the deformable bed:

$$N_{S3} \quad \frac{\dot{S}_{gen}}{\dot{S}_{gen0}} \quad \frac{C_{Di}}{C_{D0}} \frac{L_i}{L_0} \frac{U^3}{U_0^3} \tag{42}$$

Differentiation with respect to the velocity, bearing in mind all the terms of eq. (42) is velocity-dependent and looking for a minimum of N_{S3} yields:

$$\frac{C_{Di}}{C_{D0}} \frac{L_i}{L_0} \frac{U^3}{U_0^3} \quad \frac{1}{C_{Di}} \frac{\partial C_{Di}}{\partial U} \quad \frac{1}{L_i} \frac{\partial L_i}{\partial U} \quad \frac{1}{d_{ci}} \frac{\partial d_{ci}}{\partial U} \quad \frac{3}{U^3} \qquad 0 \tag{43}$$

The second term of eq. (43) provides the equation:

$$\frac{1}{C_{Di}} \frac{\partial C_{Di}}{\partial U} \quad \frac{1}{L_i} \frac{\partial L_i}{\partial U} \quad \frac{1}{d_{ci}} \frac{\partial d_{ci}}{\partial U} \quad \frac{3}{U^3} \tag{44a}$$

that leads to:

$$\ln \; C_{Di} \frac{L_i}{d_{ci}} \quad \ln \frac{A_0}{U^3} \tag{44b}$$

where A_0 is defined by the initial condition: at $U = U_0$ we have $C_{Di}(L_i/d_{ci}) = C_{D0}(L_0/d_p)$.

Hence, a substitution of A_0 and the Richardson-Zaki law into the RHS of eq. (44b) yields:

$$\frac{C_{Di}}{C_{D0}} \frac{L_i}{L_0} \frac{d_p}{d_{ci}} \quad \frac{1}{\left(\frac{\varepsilon_i}{\varepsilon_0}\right)^{3n}} \quad \frac{C_{Di}}{C_{D0}} \quad \frac{1}{1} \frac{\varepsilon_i}{\varepsilon_0} \frac{1}{\left(\frac{\varepsilon_i}{\varepsilon_0}\right)^{3n}} \frac{d_{ci}}{d_p} \tag{45a}$$

If the scaling relationship (41) is applied to the last term of eq. (45a) the results is:

$$\frac{C_{D\mathrm{i}}}{C_{D0}} \sim \frac{1}{\left(\frac{\varepsilon_{\mathrm{i}}}{\varepsilon_0}\right)^{2n}} \quad \frac{C_{D\mathrm{i}}}{C_{D0}} \quad \frac{1}{\left(\frac{U}{U_0}\right)^{2}} \tag{45b}$$

taking into consideration that order of magnitude $O[(1-\varepsilon)/(1-\varepsilon_0)] \sim 1$.

The relationship (45b) confirms the experimental results reported in [4] and it is briefly commented at the beginning of the present paper. The first form of the eq. (45a) and the consequent solution need brief comments. The substitution of eq. (41) into eq. (45a) is done by intuition since if any other exponential forms of the ratio $d_{\mathrm{p}}/d_{c\mathrm{i}} = \mathrm{f}(\varepsilon)$ exist the results may not confirm the experimental results (*i. e.* $R_c \sim 1/U^2$ $1/\varepsilon^2$) and the form (45b). Moreover, the scaling relationships (41) and (45a) ensure that ratio $N_{S3} < 1$.

Brief comments on the results developed by the entropy minimization method

Porosity/permeability relationships

The entropy minimization method provided an equation that is almost equivalent to that derived from the condition $\partial \Delta P/\partial U$ 0. In fact the second terms of eqs. (6) and (31) are practically identical. The only difference is that $\partial \Delta P/\partial U$ 0 requires a minimum of a function proportional to U^2 while the entropy minimisation looks for a minimum of a function of U^3. This difference yields different exponents $2n-2$ and $3n-4$ respectively without changes of the structures of the final relationships. At first glance this may seem reasonable, but a simple check with an average value of $n = 3$, typical for A powders, yields $2n-2 = 4$ and $3n-4 = 5$. Therefore we may state that, in general, the scaling relationship between the permeability and porosity is:

$$K \sim \varepsilon^q \tag{46a}$$

where q varies between 4 and 5. This is not only a result of the present study, but widely used scaling in models of porous media usually assumed *ad hoc* [17] as an equation of compromise, *i. e.* as a convenient parameterization for a given range of porosity/permeability variations. All the attempts to derive porosity/permeability relationship satisfying certain conditions such as constant pressure drop or minimization of the entropy yield different forms of the final equations. This is not particular crucial since the important requirement that K and $\partial K/\partial \varepsilon$ be increasing functions of porosity is satisfied in all the cases. Assuming approximately n 4 we may read the relative bed expansion as:

$$\frac{L_{\mathrm{i}}}{L_0} \quad \frac{1 \quad \varepsilon_0}{1 \quad \varepsilon_{\mathrm{i}}} \quad \frac{1 \quad \sqrt[4]{K_0}}{1 \quad \sqrt[4]{K}} \quad \frac{0.6}{1 \quad \sqrt[4]{K}} \tag{46b}$$

that allows to create a scaling relationship:

$$K \quad K\frac{L_i}{L_0} \quad 1 \quad 0.6\frac{L_0}{L_\mathrm{i}}^{4} \tag{46c}$$

This is an inexact equation that should be validated in particular cases with additional information about the particle diameter and density. However, it explains what the final target of the performed analysis is and how to apply the $K(\varepsilon)$ scaling relationships: to give engineering tools for pressure drop calculations using macroscopic data (bed depth) instead the bed porosity. The latter implies calculations of pressure drops across expanding beds through eq. (2) since in most of the technological applications the main operating parameters are: bed depth, fluid velocity and pressure drop.

Bed-to surface heat transfer coefficients

The Nusselt-Reynolds power-law relationships (22a) $\mathrm{Nu} = A\,\mathrm{Re}^{p}\,\mathrm{Pr}^{q}$ employed in heat transfer correlations use specific length scales L_i contributing both Nu and Re numbers. The ratios of these relationships for the deformed and non-deformed beds is – using the same technique as for scaling bed-to-surface heat transfer coefficients, eqs. (22a) to (23b):

$$\frac{\mathrm{Nu}_\mathrm{i}}{\mathrm{Nu}_0} \quad \frac{\mathrm{Re}_\mathrm{i}}{\mathrm{Re}_0}^{p} \quad \frac{h_\mathrm{Wi}}{h_{\mathrm{W}0}}\frac{L_\mathrm{i}}{L_0} \quad \frac{U_\mathrm{i}}{U_0}^{p} \quad \frac{L_\mathrm{i}}{L_0}^{p} \quad \frac{h_\mathrm{Wi}}{h_{\mathrm{W}0}} \quad \frac{\varepsilon_\mathrm{i}}{\varepsilon_0}^{n\ p} \quad \frac{L_\mathrm{i}}{L_0}^{p\ 1} \tag{47}$$

The RHS of the last expression of eq. (47) shows that the scaling of the heat transfer coefficients depends on the *porosity/length scale* relationships. Taking into consideration the common value of the exponent $p = 0.5$ (see [4] and [10]) and employing different relationships developed in the present study eq. (47) reads as:

For the ***Pipe equation*** (1) and the scaling relationship (41) with $L_\mathrm{i} = d_{ci}$ and $L_0 = d_\mathrm{p}$ we have:

$$\frac{h_\mathrm{Wi}}{h_{\mathrm{W}0}} \quad \frac{\varepsilon_\mathrm{i}}{\varepsilon_0}^{p} \quad (\varepsilon_\mathrm{i}^{n})^{p\ 1} \quad \frac{h_\mathrm{Wi}}{h_{\mathrm{W}0}} \quad \frac{\varepsilon^{\frac{n\ 1}{2}}}{\varepsilon_0} \tag{48a}$$

For the ***Darcy-Forchheimer equation*** (2) with $L_\mathrm{i} \quad K_\mathrm{i}^{1/2}$ and $L_0 \quad K_0^{1/2}$, and the relationship (10) the porosity/heat transfer coefficient scaling (PHCS) is:

$$\frac{h_\mathrm{Wi}}{h_{\mathrm{W}0}} \quad \frac{\varepsilon_\mathrm{i}}{\varepsilon_0}^{\frac{3}{4}n} \quad \frac{1\ \ \varepsilon_\mathrm{i}}{1\ \ \varepsilon_0}^{1} \tag{48b}$$

In both cases, the scaling relationships (48) are definitely increasing functions with the increase of the porosity (the velocity respectively). The Richardson-Zaki expo-

nent controls the "rate" of the function increase. An example how an external field can control the PHCS was demonstrated in [4, 10] through the functional relationship (5).

Limits of the porosity functions

The porosity functions developed through the present analysis are in general increasing with porosity and the initial conditions (lower limits) are imposed by the state of the non-deformed bed. The upper limits of these increasing functions are at issue. Obviously when ε 1 the porosity/permeability function (34) approaches zero that is unrealistic. Similar problem occurs with the friction factor f (see eq. 35), that is at ε 1 it approaches infinity. For instance, similar problem exists with other porosity functions (see [12] for examples), but a typical one commented in the present paper is that used in the Ergun's correlation (49) since at ε 1 the pressure drop should be zero. In order to avoid uncertainties an upper limit of the porosity should be defined from a reasonable point of view. Such an upper limit has to be defined from the maximum value of bed expansion, beyond which the bed breaks-down and vigorous particle mixing begins. Obviously, the limit ε_{crit} has to depend on both the particle properties and the gas nature contributing to the stability of the interparticle contacts. For magnetically stabilized beds this critical value is discussed below (second subsection) and an average value $\varepsilon_{crit} = 0.7$ is defined .

Intersection of asymptotes

The following analysis points out implementation of the method developed by Bejan [9] to the problems of deformable particle beds. The previous analysis considered the velocity at which the bed expansion (deformation) begins as a predetermined value. From the classical knowledge in fluidization it is well-known that this velocity can be calculated by equations representing the pressure across *via* equating them to the bed weight (per unit column cross-section area). The latter assumption comes from the fluidization practice and some oversimplified models [18] concerning calculations of minimum fluidization velocities. Let us now demonstrate how the intersection of the asymptotes technique illustrates these facts.

Bed expansion onset

For a particle bed undergoing fluidization there exist two extreme situations: fixed bed regime and fluidized bed regime. The pressure drop across the fixed bed increases with the velocity. The common practice to calculate the pressure drop is to employ the Ergun's correlation [18] since it provides reasonable results within a narrow range of porosity variations between 0.4 and 0.5 that exactly corresponds to the packings of the initial non-deformed beds:

$$\frac{\Delta P}{L} \quad 150\frac{(1 \quad \varepsilon)^2}{\varepsilon^3}\mu\frac{U}{d_{\mathrm{p}}^2} \quad 1.75\frac{(1 \quad \varepsilon)}{\varepsilon^3}\rho\frac{U^2}{d_{\mathrm{p}}} \tag{49}$$

This relation is represented by the line 1 in fig. 4a.

The second extreme assumes a constant pressure drop that usually is taken for granted as:

$$\mathrm{d}P_0 \quad \frac{G_{\mathrm{bed}}}{A_{\mathrm{bed}}} \tag{50}$$

Actually the fluidization models assuming the pressure drop equal to the bed weight per unit cross-section area state that the pressure gradient of the flowing fluid is equal to the pressure gradient produced by the body forces (gravity) of the particle bed. However, this is true if the particles are completely suspended in the fluid flow. When interparticle forces exist the stabilized bed structure hinders the particle suspension in the fluid that makes the assumption (50) physically incorrect. Usually, cohesive materials undergoing fluidization exhibit pressure drops $\mathrm{d}P_0/L < G_{\mathrm{bed}}/A_{\mathrm{bed}}$ [19] . For convenience of the further analysis we may assume that in absence of cohesive forces the pressure drop is $\mathrm{d}P_0/L$ = const., *i. e*. it is a fluid-flow independent value illustrated by the line 2 in fig. 4a.

The application of the intersection of asymptotes method yields the line 3-0 that points an optimum of the pressure drop with respect to the velocity as a controlling parameter and coinciding with the minimum fluidization point. Therefore the formalism of the method leads to a well-know result developed independently on the base of huge ex-

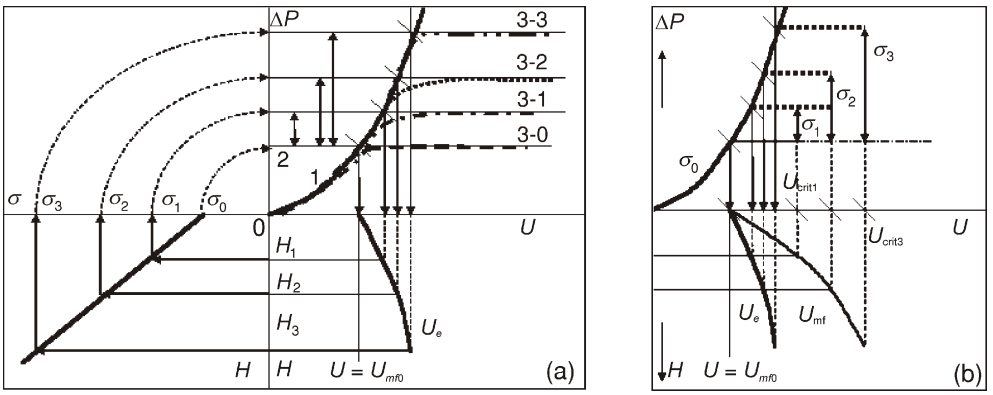

Figure 4. Intersection of asymptotes method – graphical explanations

(a) Determination of the minimum fluidization point (optimal pressure drop) – axial field; ΔP-U chart – main drawing explaining the intersection of asymptotes at the minimum fluidization point, σ-H chart – induced magnetic cohesion as a function of the magnetic field intensity, U-H chart – resultant phase diagram of the bed;

(b) Determination of the break-down points of the expanding beds at the intersection of the horizontal asymptote and a vertical line corresponding to U_{crit}

perimental data. Further, from the standpoint of optimization of the pressure drop across the bed, the minimum fluidization point can be considered as a point where the particulate system starts to re-organize itself in order to achieve an internal structure minimizing the pressure loses. This is a well-known statement from the fluidization literature, but it is mainly explained by words and never supported by results developed from general mechanical or thermodynamic principles. The results developed here from the standpoint of entropy minimization and optimization of the pressure losses demonstrates that the fluidization onset, or at least the bed expansion, of cohesive powders is a performance of bed self-optimization through particle rearrangements.

The graphical solution, just commented, corresponds to a case of non-cohesive particles and interparticle contacts stabilized by a pressure (normal stress) produced by the weight of solids. If additional interparticle forces take place, such as cohesion or electrostatic forces, they will augment the normal stresses at the interparticle contacts. The latter has to be explained to the readers non-experienced in powders mechanics. The cohesion Co is a residual normal stress (the tensile strength) in absence of shear stresses according to the Coulomb's equation of dry friction [19, 20]:

$$\tau = \mathrm{Co} + \sigma \mathrm{tg}\varphi \tag{51}$$

Therefore, by summing up the normal stresses in the powder body produced by the weight and the additional interparticle forces we obtain a second pressure drop extreme that moves up as a line parallel to the velocity axis (see the doted lines approximating the pressure drop curves in fig. 4a. Hence, the intersections of the asymptotes yield new optimal points that move to the left, *i. e*. to higher fluid velocities. This is a reasonable result since stronger interparticle contacts require stronger drag forces (high pressure loses, *i. e.* higher fluid velocities) to destroy the bed packing. In the case of magnetically stabilized beds this upward shift of the plateaux of the pressure drop curves with the increasing field intensity has been proved experimentally [2]. Moreover, the induced magnetic cohesion is proportional (almost linearly) to the field intensity applied [20] (see the left-lower quadrant of fig. 4a) as:

$$\mathrm{Co}^{\mathrm{M}} = a_C H + \mathrm{Co} \tag{52}$$

where a_C is a factor of proportionality depending on the field lines orientation (in transverse fields the values of a_C are higher that in axial fields); Co is the native bed cohesion in absence of an external field.

Therefore, if we try to illustrate all these facts the resulting drawing is in the lower-right quadrants in fig. 4a representing the lower bound of the stabilized bed by the velocity U_e. Obviously, the increase of the interparticle forces results in the velocity U_e (greater than U_{mf0}) at which the cohesionless bed begins to rearrange its packing. It was proved (see [2]) that in axial fields the ratio U_e/U_{mf0} might reach values of about 1.12 depending on the magnetic properties of the materials. In a transverse field (see subsection brief comments) U_e/U_{mf0} may achieve values in the range of 1.2-1.5 (see for more information in [2]).

Break-down of the expanded bed (fluidization onset)

The second asymptote commented in the previous point defines a flat curve that is not bounded to the right as the fluid velocity increases. In order to define the point where the bed expansion will stop we need additional information about the bed stability or more precisely about the bed rheology. Actually the bed stability depends on type of the packing and the number of the interparticle contacts per unit volume. From the point of view developed in the present paper the latter implies that the bed stability decreases with increasing bed porosity. This is a general fact observed not only in non-magnetic beds but in beds controlled by external fields. The latter cases are typical examples how the external field intensity can control the "width "of the plateaux of the pressure drop curves. It may suggest that there is a critical value at which the bed breaks-down. This critical porosity might depend on the stability of the interparticle contact and the ability of the bed to be deformed by the fluid drag forces. It was demonstrated experimentally [21] that beds stabilized by external axial fields exhibit maximum relative bed expansions in the range $E_{max} = 0.5\text{-}0.6$ irrespective of the particle magnetic properties and field intensities applied. For instance, the increase of the interparticle forces (*i. e.* stronger fields) results in slow bed expansions with increasing fluid velocity, while the decrease of the interparticle forces yields steeper bed expansion curves. The relative bed expansion E is defined as [21]:

$$E \quad \frac{L \quad L_0}{L_0} \quad \frac{L}{L_0} \quad 1 \quad \frac{1 \quad \varepsilon_0}{1 \quad \varepsilon} \quad 1 \tag{53}$$

Consequently, the maximum values of $E_{max} = 0.5$ and $E_{max} = 0.6$ correspond to critical porosities $\varepsilon_{crit} = 0.7$ and $\varepsilon_{crit} = 0.68$ respectively with $\varepsilon_0 = 0.5$. If the initial porosity is assumed as $\varepsilon_0 = 0.4$ the corresponding critical porosities are $\varepsilon_{crit} = 0.73$ and $\varepsilon_{crit} = 0.75$ respectively. Thus, for convenience we may recognize an average value $\varepsilon_{crit} = 0.7$, which will help us to develop further the method. Since the Richardson-Zaki low is valid the critical porosity ε_{crit} defines the fluid velocity of bed break-down, namely:

$$U_{crit} = U_t \varepsilon^n \tag{54}$$

More precisely, the Richardson-Zaki law plays a role of a rheological equation employing macroscopic values only. The values of n decrease with the field intensity – see eq. (5), so lower values of n, higher critical velocities U_{crit} since the velocity U_t is a constant *independent of the field intensity*. For instance, at $n = 3$, that is an average value for non-magnetic beds, the critical velocity is defined as $U_{crit} = U_t \varepsilon^n = 0.34 U_t$ while for $n = 2$ (magnetized bed, see [2]) the result is $U_{crit} = U_t \varepsilon^n = 0.49 U_t$. This physical explanation is illustrated by the drawings in fig. 4a and b, and fig. 5. The final result (the lower right-part of fig. 4b) is the bed phase diagram.

Brief comments

The intersection of the asymptotes method (IAM) explained qualitatively the results obtained from many experiments (see [2, 21]) through a simple optimisation proce-

dure. The main issue is that the resulting curve defines the optimal bed pressure drop at the minimum fluidization point (*i. e.* the onset of bed deformation) as well the shape of the pressure drop curve beyond this point. Further, the intersections of the pressure drop curves with the vertical asymptotes, predetermining the upper critical velocities (porosities), define the break-down points of the expanded beds. The envelops of the critical points are the curves $U_e = \mathrm{f}(H)$ and $U_{mf} = \mathrm{f}(H)$ (since $U_{\mathrm{crit}} = U_{mf}$ in accordance with the accepted terminology [2]) consequently defining the well-know phase diagrams. In the context of the present paper the second asymptote (the pressure drop plateau) can be modelled by the Darcy-Forchheimer equation as well. In this case the Richardson-Zaki law and scaling estimates such as eqs. (10a and b) and (34a and b) or more simply eq. (46a) can be used. Numerical experiments testing these suggestions are beyond the scope of the present study.

The method can be applied also to cases of magnetically stabilized beds in fields with orientations different from axial. These cases are beyond the objectivities of the present paper, but short comments will outline the idea. The general case (non-axial fields) is that the derivative $\partial(\Delta P)/\partial$ 0, so different functional relationships $\partial(\Delta P)/\partial U \quad \mathrm{f}_p(U)$ may be suggested. The function $\mathrm{f}_p(U)$ decreases with the velocity and defines the negative differential resistance of the bed [4]. It was mentioned in [4] that a linear functional relationship may be used, *i. e.* $\mathrm{f}_p(U) = -mU$ approximates the pressure drop across MSB in transverse fields (see [2, 22]). The function $\mathrm{f}_p(U)$ defines the second

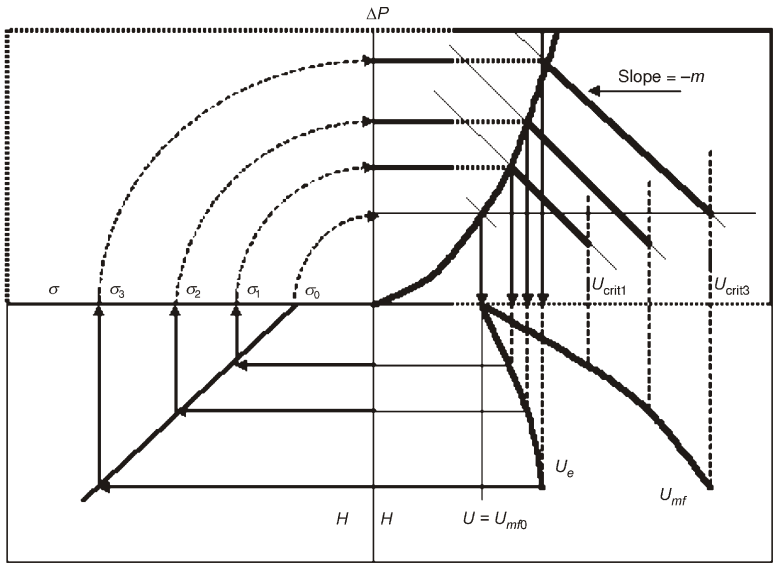

Figire 5. Application of the intersection of asymptotes method in cased of beds stabilized by non-axial fields. The second asymptote is not parallel to the velocity axis, but it has a negative slope *–m*. The lower right chart is the resultant phase diagram

extreme of the pressure drop beyond the onset of deformation process. The drawing in fig. 5 illustrates the application of the intersection of the asymptotes method in these cases. If a different functional relationship unlike linear one is used this does not alter the validity of the method but the shape of the second asymptote (extreme) will be changed with a consequent effect on the determination the critical velocities U_{crit}.

Standpoint

The main fact coming from experimental practice, used in this study, is the fluid-independent pressure drop exhibited by fluidized beds with cohesive forces. The fact is assumed here as undisputable one and it is used to find answers to several questions that can be generalized as follows:

- If the fluid-independent pressure drop exists, what should be the relationships of the parameters of a certain model describing the fluid flow through the bed? Since a range of models can be employed, the question has a variety of answers. However, the main outcome of the present paper is – the bed tries to minimize it hydraulic resistance and formally the fluid flow length scales increases with the bed porosity. In other words, such behaviour may be formulated philosophically as a "self-adaptation" or a "self-organization" of the granular medium as a reaction of the fluid flow action on it.
- In the classical textbooks on fluidization explanations based on the balance between the pressure gradient and the gradient of the body forces, *i. e.* – grad$P = (\rho_s - \rho_g)(1 - \varepsilon)$g exist. The latter could be accepted as a satisfactory explanation in cases of completely homogenous suspensions of particles in fluidizing flows. However, states as the expansion of A powders and the behaviour of field-assisted beds cannot be answered in a such straightforward way. Despite this, we accept the fluid-independent pressure drop of a class of fluidized beds with significant interparticle forces as a natural phenomenon and try to derive engineering equations. The answer of the general question, why the granular medium reacts in such manner to the action of the fluid flow still remains unanswered and it is a challenging problem, but beyond the objectivities of the present paper.

Conclusions

Too many comments and different analysis were performed through the development of the study. The ideas and the author's point of view are explained in every particular section of the paper. The conclusions are short and the main issues are outlined:

- The principle question about the permeability/porosity functional relationship in case of fluid-driven deformation of particle beds has solutions that may be derived through several approaches- direct analysis of equations, mechanistic equivalent models and entropy generation minimization method.
- The Darcy-Forchheimer equation in its particular form with both terms related to the permeability is a tool providing reasonable theoretical results. The present analysis

yields an explicit formula upon conditions imposed by the Richardson-Zaki law and the fluid-independent pressure drop. Besides, the approach is general and can be applied to cases of fluid-dependent pressure drops if $\Delta P/L = f(U)$ functional relationships are known.

- Porous media may be studied through equivalent hydraulic structures adequately designed to represent the basic features at issue. The development of the idea of Lage from his slot model towards the equivalent channel model of deformable bed is a useful and yields surprisingly sound results confirming the physical facts as the results derived through direct analysis of the Darcy-Forchheimer equation.
- The entropy minimization approach was tested with the Darcy-Forchheimer equation in a simple case without heat transfer. This was done especially in order to demonstrate the validity of the method and its implicit link to the direct analysis of the Darcy-Forchheimer equation outlined in the previous point.
- The short excursions to apply the results from the permeability/porosity and friction factor/porosity studies to bed-to-surface heat transfer with immersed bodies provide rational results explaining experimental facts (see more information in [4, 10]).
- The intersection of the asymptotes method was applied to fluidized bed formally different from the objects for which it was originated. However, actually from an intimate point of the physics the problem, it is an optimization of the flow resistance of the object under consideration.
- Finally, but not at least it is clear that the *synergetic effect* of applications of methods developed in one branch of the science to other formally distinct objects provides new results. The main issue of such approaches is the use of the fundamental knowledge. The applications may be different, but the fundamental ideas of the science remain and are inspiring "fuels" driving the search of basic laws of the nature and developing new practical results.

Nomenclature

A_{bed} – cross-sectional area of the bed, [m^2]
C_D – friction factor of a deformed bed in accordance with eq. (1)
C_{Di} – friction factor of a deformed bed
C_{D0} – friction factor of the initial bed at $U = U_{e1}$, in accordance with eq. (1)
C_i – friction factor of a deformed bed
C_p – specific heat, [J/kgK]
C_0 – friction factor of a initial bed
Co – cohesion normal stress, [N/m^2]
Co^M – cohesion normal stress induced by the magnetic field, [N/m^2]
D – tube (pipe or column) diameter – see the context , [m]
d_{ci} – length scale of a deformed bed
d_p – particle diameter, [m]
d_s – slot aperture or core cylinder diameter, [m]
F – inertia factor of Forchheimer's equation, [–]
f – friction factor, [–]
G – bed weight, [N]

g – acceleration of gravity, [m/s^2]
H – magnetic field intensity, [A/m]
– (=h/d), dimensionless channel length, [–]
h – channel aperture, [m]
h_W – wall-to-bed heat transfer coefficients, [W/m^{2}K]
K – porous bed permeability, [m^2]
L – length, [m]
L_i – current bed length, [m]
L_0 – initial bed length, [m]
Ms – magnetization at saturation, [A/m]
$\dot{m}$ – mass flow rate, [kg/m^{2}s]
N_S – ratio of entropy generation rates, [–]
Nu – (=$h_W l_0/k$), Nuselt number (see the context for the specifically defined length scale l_0 and conductivity k)
n – Richardson-Zaki exponent of a magnetizable bed, [–]
n_0 – Richardson-Zaki exponent of a non-magnetic bed, [–]
P – pressure, [Pa]
Pr – (=$\mu c_p/k$), Prandtl number, [–]
ΔP – pressure drop across the bed, [Pa]
p – pre-factor in eq. (5), [–]
$\dot{Q}$ – total heat transfer rate, [W]
q – surface density of the heat flux, [W/m^2]
Re – (= $U_0 l_0/\nu$), Reynolds number (see the context for the specifically defined length l_0 and velocity U_0 scales)
Re_p – (=$\rho_p U d_p/\mu_g$), particle Reynolds number, [–]
$\dot{S}$ – entropy generation, [W/K]
s – entropy, [J/kgK]
T – temperature, [K]
U – superficial fluid velocity, [m/s]
$U(X,Y)$ – dimensionless velocity in eq. (12), [–]
U_e, U_{e1} – velocity at the onset of the stabilized bed, [m/s]
U_{crit} – velocity at the break-down of the stabilized bed, [m/s]
U_{mf0} – minimum fluidization velocity in absence of magnetic field, [m/s]
U_{se} – velocity at the onset of the stabilized bed corresponding to the structure of the equivalent channel model, [m/s]
U_t – particle terminal velocity, [m/s]
$\overline{u_i}$ – superficial velocity for the channel – fig. 2b, [m/s]
$\overline{u_s}$ – superficial velocity for the slot – fig. 2a, [m/s]
V_{bed} – bed volume, [m^3]
V_0 – void volume, [m^3]
X – (=x/d), dimensionless lateral coordinate, [–]
x – axial co-ordinate (parallel to fluid flow and field lines, [m]
Y – (=y/d), dimensionless longitudinal coordinate, [–]

Greek letters

ε – porosity, [–]
ε_i – porosity of the deformed bed, [–]
ε_0 – porosity of the initial (non-deformed) bed, [–]
$\Delta\varepsilon$ – porosity increment due to the bed deformation, [–]

μ – fluid dynamic viscosity, [Pa·s]
ν – fluid kinematic viscosity, [m^2/s]
ρ – density, [kg/m^3]
σ – normal stress, [N/m^2]
τ – shear stress, [N/m^2]
Φ – porosity function defined by eq. (4)
φ – angle of internal friction (granular medium), [deg]

Subscripts

i – deformed bed
0 – initial (non-deformed) bed
g – gas
p – particle
s – solid phase
W – wall

Abbreviations

LHS – Left hand side
RHS – Right hand side
MFAF – Magnetic field assisted fluidization
MSB – Magnetically stabilized bed

References

[1] Geldart, D., Types of Gas Fluidization, *Powder Technology, 7* (1973), 2, pp. 285-292
[2] Hristov, J., Magnetic Field Assisted Fluidization – A Unified Approach. Part 1. Fundamentals and Relevant Hydrodynamic of Gas-Fluidized Beds, *Reviews in Chemical Engineering, 18* (2002), 4-5, pp. 295-509
[3] Hristov, J. Y., Expansion Scaling and Elastic Moduli of Gas-Fluidized Magnetizable Beds, in: Current Issues on Heat and Mass Transfer in Porous Media, NATO ASI "Emerging Technologies and Techniques in Porous Media" (Eds. D. Ingham, A. Bejan, E. Mamut, I. Pop), Kluwer, Dordrecht, The Netherlands, 2004, pp. 477-489
[4] Hristov, J. Y., Friction Factors and Internal Flow Length Scales of Gas-Solid Magnetically Stabilized Beds in Axial Fields: Scaling and Applications to Bed-to-Surface Heat Transfer, *Thermal Science, 9* (2005), 1, pp. 73-98
[5] Hristov, J., Magnetic Field Assisted Fluidization – A Unified Approach. Part 2. Solids Batch Gas-Fluidized Beds: Versions and Rheology, *Reviews in Chemical Engineering, 19* (2003), 1, pp. 1-132
[6] Beavers, G. S., Wilson, T. A., Masha, B. A., Flow Through a Deformable Porous Material, *J. Appl. Mech, 42* (1975), 9, pp. 598-602
[7] Beavers, G. S., Sparrow, E. M., Compressible Gas Flow through a Porous Material, *Int. J. Heat Mass Transfer, 14* (1971), 11, pp. 1855-1899
[8] Bejan, A., Advanced Engineering Thermodynamics, John Wiley and Sons, New York, USA, 1989
[9] Bejan, A., Shape and Structure, from Engineering to Nature, Cambridge University Press, Cambridge, UK, 2000
[10] Hristov, J. Y, Heat Transfer between Deformable Magnetic Beds and Immersed Surfaces: Cases of Gas-Fluidized Beds, *Proceedings*, ASME-ZSIS International Thermal Science Seminar ITSS II, Bled, Slovenia (Eds. A. Bergles, I. Golobic, Cr. Amon, A. Bejan), 2004, pp. 267-274
[11] Cheng, P., Hsu, C. T., Chowdhury, A., Forced Convection in the Entraance Region of a Packed Channel with Asymmetric Heating, *J. Heat Transfer, 110* (1988), 11, pp. 946-954
[12] Dullien, F. A. L., Porous Media – Fluid Transport and Pore Structure, Academic Press, New York, USA, 1979

[13] Carman, P. C., , Fluid Flow through Granular Beds, *Trans. Inst. Chem. Engng.,15* (1937), 1, pp. 150-166
[14] Denn, M. M., Process Fluid Mechanics, 1st ed., Prentice-Hall, Englewood Cliffs, NJ, USA, 1980
[15] Naakteboren, C., Krueger, P. S., Lage, J. L., Limitations of Darcy's Law of Inlet and Exit Pressure-Drops, *Proceedings*, ICAPM 2004, Applications of Porous Media (Eds. A. H. Reis, A. F. Miguel), Evora, Portugal, 2004, pp. 1-7
[16] Lage, J. L., The Fundamental Theory of Flow through Permeable Media from Darcy to Turbulence, in: Transport in Porous Media (Eds. D. B. Ingham, I. Pop), Pergamon Press, Oxford, UK, pp. 1-30
[17] Spiegelman, M., Flow in Deformable Porous Media, I: Simple Analysis, *J. Fluid. Mechanics, 247* (1983), 1, pp. 17-38
[18] Kunii, D., Levenspiel, O., Fluidization Engineering, 2nd ed., Butterworth-Heinemann, Boston, PA, USA, 1991
[19] Baerns, M., Effect of Interparticle Adhesive Forces on Fluidization of Fine Particles, *Ind. Eng. Chem. Fund., 5* (1966), 4, pp. 508-516
[20] Brown, R. L., Richards, D., Principle of Powder Mechanics, Pergamon Press, London, 1970
[21] Hristov, J., Magnetic Field Assisted Fluidization – A Unified Approach, Part 2. Solids Batch Gas-Fluidized Beds: Versions and Rheology, *Reviews in Chemical Engineering, 19* (2003), 1, pp. 1-132
[22] Penchev, I., Hristov, J., Behaviour of Fluidized Beds of Ferromagnetic Particles in an Axial Magnetic Field, *Powder Technology, 61* (1990), 3, pp. 103-118
[23] Penchev, I. P., Hristov, J. Y., Fluidization of Ferromagnetic Particles in a Transverse Magnetic Field, *Powder Technology, 62* (1990), 1, pp. 1-11

Author's address:

J. Y. Hristov
Department of Chemical Engineering
University of Chemical Technology and Metallurgy
1756 Sofia, 8, Kl. Ohridsky Blvd., Bulgaria

E-mail: juh@uctm.edu; jordan.hristov@mail.bg
Website: http://hristov.com/jordan

Paper submitted: December 2, 2004
Paper revised: February 4, 2005
Paper accepted: February 13, 2006